J. Biochem. 2009;146(5)651–657
doi:10.1093/jb/mvp110

Importance of the Hydrogen Bonding Network Including Asp52 for Catalysis, as Revealed by Asn59 Mutant Hen Egg-white Lysozymes

Toyoyuki Ose[1], Kimiko Kuroki[1], Masaaki Matsushima[2], Katsumi Maenaka[1,*] and Izumi Kumagai[3]

[1]Medical Institute of Bioregulation, Kyushu University, Higashi-ku, Fukuoka, 812-8582; [2]Aino University, 4-5-4 Higashi-ohta, Ibaragi, Osaka 567-0012; and [3]Department of Biochemistry and Engineering, Graduate School of Engineering, Tohoku University, Aoba-ku, Sendai 980-77, Japan

Received April 27, 2009; accepted June 29, 2009; published online July 15, 2009

In the catalysis of sugar hydrolysis by hen egg-white lysozyme, Asp52 is thought to stabilize the reaction intermediate. This residue is involved in the well-ordered hydrogen bonding network including Asn46, Asp48, Ser50 and Asn59 on the anti-parallel β-sheet, designated as a 'platform', on which the substrate sugar sits. To reveal the role of this hydrogen bonding network in the hydrolysis, we characterized Asn59 mutants by biochemical and crystallographic studies. Surprisingly, the introduction of only a methylene group by the Asn59Gln mutation markedly reduced the bacteriolytic activity and abolished the hydrolytic activity towards the synthetic substrate, PNP-$(GlcNAc)_5$. A similar result was also obtained with the Asn59Asp mutant. The crystal structure of the Asn59Asp mutant in complex with the substrate analogue revealed that, as in the wild-type, the $(GlcNAc)_3$ was bound in the A–B–C subsites. The reduced activity would be caused by subtle changes in the side-chain orientations as well as the electrostatic characteristics of Asp59, resulting in the rearrangement of the hydrogen bonding network of the platform. These results suggest that the precise locations of these 'platform' residues, maintained by the well-ordered hydrogen bonding network, are crucial for efficient hydrolysis.

Key words: catalytic activity, lysozyme, protein–carbohydrate interactions, protein engineering, X-ray crystallography.

Abbreviations: PNP, *p*-nitrophenyl; GlcNAc, N-acetyl-β-D-glucosaminine (PNP-G1cNAc); MurNAc, N-acetylmuramic acid; SDS, sodium dodecyl sulfate; HPLC, high pressure liquid chromatography; NMR, nuclear magnetic resonance.

Hen egg-white lysozyme catalyses the hydrolysis of β-1,4 glycosidic bonds of alternating copolymers of GlcNAc and MurNAc[1] in bacterial cell walls as well as the homopolymer of GlcNAc, chitin (*1–3*). Hen egg-white lysozyme has been extensively studied by functional and structural analyses (*4*), and has six binding subsites for the sugar residues, termed A–F (*5*, *6*). Catalytic models of sugar hydrolysis by hen egg-white lysozyme were proposed independently by Phillips (*7*) and Koshland (*8*). The first step is well-understood, and involves Glu35, which possesses an unusual pKa, protonating the oxygen connecting the sugar residues D and E. On the other hand, in the next step, the role of Asp52, which was proposed to stabilize the oxocarbonium ion of the intermediate state in the hydrolysis, still remains unclear. Kuroki *et al*. (*9*) reported the crystal structure of the mutant Asp52Glu complexed with $(GlcNAc)_6$, which clearly revealed the covalent bond between the Oε atom of Glu52 and the C1 atom of sugar D of the resultant hydrolysis product $(GlcNAc)_4$. However, it seems unlikely that the wild-type forms the covalent bond during catalysis, because Asp52 is still too far from the C1 of sugar D. Moreover, Vocaldo *et al*. (*10*) detected the covalent intermediate of the Glu35Gln mutant lysozyme with $(GlcNAc)_2GlcF$ through Asp52. On the basis of a comparison with other β-glycosidases, they proposed that the anomer-retaining β-glycosidases adopt the general catalytic mechanism, including the formation of the covalent intermediate.

Although Asp52 has a normal pKa, it participates in the well-ordered hydrogen bonding network called the 'platform' (*5*), which includes Asn46, Asp48, Ser50 and Asn59. As expected, several previous studies showed that the replacement of Asp52 reduced the hydrolytic activity to <5% of the wild-type. However, except for the studies of the Asn46 mutant, which also showed a reduction of the hydrolytic activity (*11*), only limited information is available about the role of this hydrogen bonding network in the hydrolysis. To clarify the functional and structural relevance of the platform hydrogen bonding network on the activity, we focused on the residue Asn59, which directly interacts with the catalytic residue Asp52, and analysed the mutants Asn59Asp and Asn59Gln by biochemical and crystallographic methods.

*To whom correspondence should be addressed. Tel/Fax: +81-92-642-6998, E-mail: kmaenaka-umin@umin.net
Correspondence may also be addressed to Dr Izumi Kumagai. Tel: +81-22-795-7274, Fax: +81-22-795-6164,
E-mail: kmiz@mail.tains.tohoku.ac.jp

EXPERIMENTAL PROCEDURES

Preparation of the Mutant Lysozymes and Analyses of their Enzymatic Activity—The Asn59 mutant hen lysozyme cDNAs used in this study were prepared by site-directed mutagenesis, as described previously (*12*, *13*). The mutations were confirmed by DNA sequencing analyses. The Asn59 mutants were expressed in *Saccharomyces cerevisiae* AH22, and were purified by two steps of cation-exchange chromatography (S-Sepharose and MonoS columns), using a method similar to that described previously for the wild-type and mutant lysozymes (*12*, *13*). The size and homogeneity of the purified mutant proteins were analysed by SDS–PAGE.

The bacteriolytic activity of the wild-type and mutants was measured by the standard method described in our previous reports (*12*, *13*). Lysozyme was added to a 1-ml suspension of *M. lysodeikticus* cells in 50 mM sodium phosphate buffer (pH 6.2) at 25°C. The decrease in the absorbance at 540 nm after 1 min was measured and compared between the wild-type and mutant lysozymes. Similarly, the hydrolytic activity towards the synthetic substrate $(GlcNAc)_5$-PNP of the wild-type and mutants was determined by the method described previously (*12*, *13*). $(GlcNAc)_5$-PNP (0.26 mM) was incubated with 1 mg of each lysozyme at 37°C, in 50 ml of 50 mM sodium acetate buffer, pH 5.0. The reaction products were analysed by HPLC, using a YMC-Pac A014 column.

Crystallization, X-ray Data Collection and Structural Determination—The crystallization of the Asn59Asp lysozyme mutants with and without a substrate analogue, $(GlcNAc)_3$, was achieved with a protocol similar to that described previously (*14*). The crystals were obtained with 10–15% NaCl (w/v) in sodium-acetate buffer (pH 4.7) at 20°C. The crystallographic data statistics are summarized in Table 1, and show that the unit cell parameters are almost identical to those of the wild-type enzyme (*14*). Diffraction data were collected at 4°C by an automated oscillation camera system (DIP320) equipped with a cylindrical Imaging Plate on a rotating anode generator (M18X) operated at 50 kV, 90 mA, with CuKα radiation. The crystals were oscillated by 2° for each frame around an appropriate diagonal axis in the (h, k, 0) plane. For each crystal, diffraction data sets were collected in 50 frames, with negligible radiation damage during the experiment. The exposure time per frame was 50 min. The diffraction intensities were evaluated with the WELMS program system (*15*), and were processed using the PROTEIN program package (*16*).

We used the coordinates of the wild-type hen egg-white lysozyme (*14*) as an initial model for the structure determination. The atomic parameters were refined using the CNS (*17*) and Refmac5 (*18*) programs. The mutated residue and the bound substrate saccharide were carefully fitted to the electron densities, using COOT (*19*). Coordinates and structure factors of the both ligand free and complex structures have been deposited in the Protein Data Bank (PDB ID 3A3R and 3A3Q).

Table 1. **Data collection and refinement statistics.**

	Asn59Asp mutant	Asn59Asp mutant–$(GlcNAc)_3$ complex
Data collection		
Space group	$P4_32_12$	$P4_32_12$
Cell dimensions		
a, b, c (≈)	79.2, 79.2, 38.6	78.7, 78.7, 38.6
Resolution (≈)	50–1.90 (1.95–1.90)	50–2.00 (2.05–2.0)
R_{sym} or R_{merge}	0.084	0.098
Redundancy	4.6	3.9
Completeness[a] (%)	83.1 (49.1)	76.6 (55.9)
Refinement		
Resolution (≈)	20–1.90	50–2.00
No. of reflections	8438	6611
R_{work}/R_{free}[b]	0.202/0.249	0.205/0.287
No. of atoms		
Protein	1,001	1,001
Ligand/ion	0	43
Water	107	96
B-factors		
Protein	15.3	9.22
Ligand/ion		22.1
Water	26.8	26.1
RMSDs		
Bond lengths (≈)	0.009	0.011
Bond angles ($\int$)	1.145	1.339

[a]Values in parentheses are for the highest resolution shells. [b]R_{free} factors were calculated for 10% randomly selected test sets that were not used in the refinement.

RESULTS

Preparation of Asn59 Mutants and their Hydrolytic Activity—The Asn59Gln and Asn59Asp mutants were constructed and expressed as described in the EXPERIMENTAL PROCEDURES section. The yields for these mutants were roughly 100–200 μg l culture. For further biochemical studies and crystallization, purification by Mono S chromatography was performed at the final stage. Figure 1A shows representative results of the hydrolytic activities of both Asn59Asp and Asn59Gln mutants towards the *M. lysodeikticus* bacterial cell walls. The presence of only one additional methylene group on residue 59 (Asn59Gln) significantly reduced the bacteriolytic activity, and the Asn59Asp mutation further increased the detrimental effects. Moreover, the hydrolytic activity towards the synthetic substrate $(GlcNAc)_5$-PNP was remarkably decreased for the Asn59Gln mutant, and was hardly detectable for the Asn59Asp mutant (Fig. 1B). Therefore, residue 59 plays a key role in the efficient hydrolysis of the natural product, bacterial cell walls, as well as the synthetic GlcNAc oligomer.

Crystal Structures of the Asn59Asp Mutant Lysozymes—To identify the structural basis of the reduced hydrolytic activities of these Asn59 mutants, we performed X-ray crystallographic analyses of the Asn59Asp mutant lysozyme with and without the substrate analogue, $(GlcNAc)_3$. Unfortunately, the crystals of the Asn59Gln mutant could not be obtained.

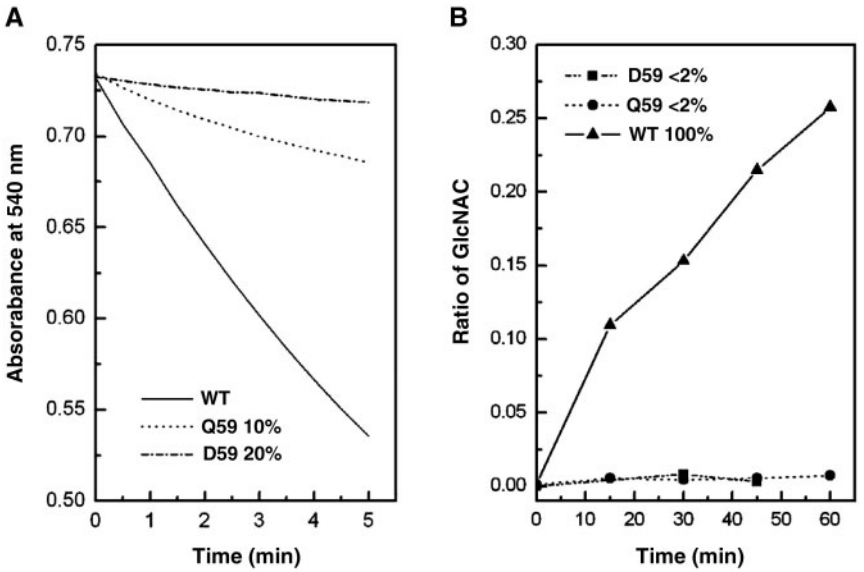

Fig. 1. **(A) Bacteriolytic activities of the wild-type and Asn59 mutant lysozymes.** The lines indicate the enzymes as follows: (*1*) solid (wild-type), (*2*) dashed (Gln59) and (*3*) dotted (Asp59). (B) Hydrolytic activities of the wild-type and Asn59 mutant lysozymes towards PNP-$(GlcNAc)_5$. (*1*) Triangles (wild-type), (*2*) circles (Gln59) and (*3*) squares (Asp59).

The crystal data and the final refinement parameters and statistics are summarized in Table 1. The crystals of the Asn59Asp mutant protein and its complexes were isomorphous with those of the wild-type enzyme. The resolution limits of the diffraction for the free and complex forms were 1.9 Å and 2.0 Å, respectively. The final (2*F*o–*F*c) map for the sugar substrate analogue, $(GlcNAc)_3$, is shown in Fig. 2A. Each of the refined models possesses about 100 water molecules.

The overall structures of the mutant protein in both the free and complex forms were almost identical to that of the wild-type protein determined previously by our group (Fig. 2B). The RMSDs of the main-chain atoms (N, Cα, C and O) in comparison with wild-type lysozyme were 0.20 Å for both the Asn59Asp mutant and its $(GlcNAc)_3$ complex.

Binding Modes of GlcNAc Residues—The final model of the Asn59Asp–$(GlcNAc)_3$ complex is similar to the wild-type–$(GlcNAc)_3$ model. The bound $(GlcNAc)_3$ molecule fits well into the strong electron densities (Fig. 2A), showing that $(GlcNAc)_3$ is bound in the binding subsites, A–B–C, as observed in the wild-type. This is in contrast with our previous studies, which revealed the shift of the binding modes from A–B–C to B–C–D, in both Trp62Tyr and Trp62Phe mutants (*14*), and the unusual binding mode, L1–L2, in Trp62Gly and Asp101Gy mutants (*20*). Trp62 forms a stacking interaction with the hydrophobic face of the sugar in site B, which is a general feature often observed in protein–carbohydrate interactions, while Asp101 interacts with the same sugar via a hydrogen bond. Thus, these conversions of subsite B have remarkable effects on the binding modes of the substrate sugars. The enzyme–substrate interactions between the wild-type enzyme–$(GlcNAc)_4$ complex and the Asp59 mutant–$(GlcNAc)_3$ complex are compared in Fig. 3A. These results showed that most of the possible hydrogen bonds between the protein and the

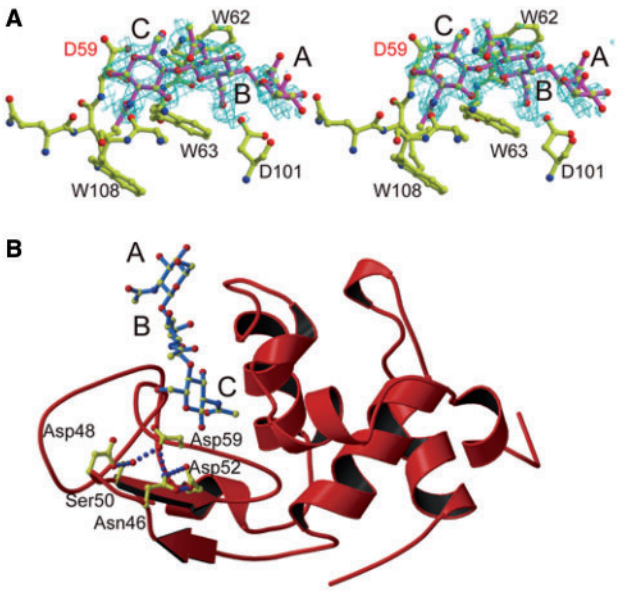

Fig. 2. **Overall structure of the Asn59Asp mutant–$(GlcNAc)_3$ complex.** (A) Stereo view of the 2*F*o–*F*c electron density map, contoured at 1σ, showing the $(GlcNAc)_3$ in subsites A–C. Protein residues are coloured yellow and $(GlcNAc)_3$ is magenta. (B) The ribbon model presentation of the Asn59Asp mutant–$(GlcNAc)_3$ complex structure. The $(GlcNAc)_3$ molecule (blue) and the 'platform' residues (yellow) are shown in ball-and-stick models. The hydrogen bonding network on the 'platform' residues is indicated by blue dotted lines.

carbohydrate are commonly used in each complex (Fig. 4). These include the hydrogen bonds between (i) the main-chain nitrogen atom of Asp59 and the O7 atom of the N-acetyl group of the sugar residue in site C, (ii) the nitrogen atom of the indole ring of Trp63 and the O3 atom of the sugar residue in site C,

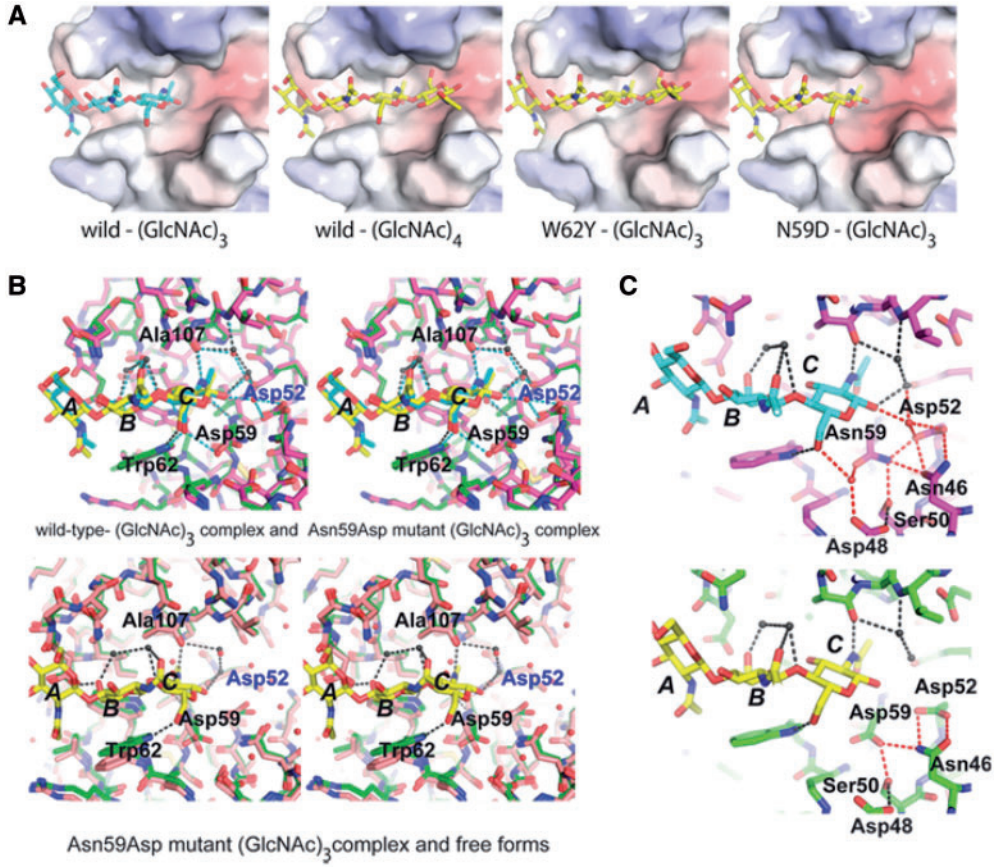

Fig. 3. **Interactions between lysozyme and the bound GlcNAc oligomer around the active site.** (A) Protein (surface models, with the colour showing the electrostatic charge distribution) and bound $(GlcNAc)_n$ of (i) wild-type–$(GlcNAc)_3$ complex, (ii) wild-type–$(GlcNAc)_4$ complex, (iii) Trp62Tyr mutant–$(GlcNAc)_3$ complex and (iv) Asn59Asp mutant–$(GlcNAc)_3$ complex. In the wild-type, the $(GlcNAc)_3$ and $(GlcNAc)_4$ molecules are bound in subsites A–B–C and A–B–C–D, respectively. The Asn59Asp mutant bound the $(GlcNAc)_3$ molecule in subsites A–C, but the Trp62Tyr mutant bound the $(GlcNAc)_3$ molecule in two modes, A–C and B–D, resulting in the electron density covering subsites A–D. (B) Stereo views of the detailed interactions around residue 59. Top: wild-type (pink); $(GlcNAc)_3$ (light blue) complex structure and Asn59Asp mutant (green); $(GlcNAc)_3$ (yellow) complex structure. Bottom: Asn59Asp mutant (green); $(GlcNAc)_3$ (yellow) complex and free form (pink) structures. (C) The hydrogen bonding networks through the 'platform' residues in the wild-type–$(GlcNAc)_3$ complex structure (top) and the Asn59Asp mutant–$(GlcNAc)_3$ complex (bottom) structure. Water molecules shared in both structures are depicted by black spheres, whereas those only observed in the wild-type–$(GlcNAc)_3$ complex are red. Common hydrogen bonds are depicted as dashed black lines, whereas the distinctive ones in each of the structures are depicted as red dashed lines.

(iii) the nitrogen atom of the indole ring of Trp63 and the O6 atom of the sugar in site C, (iv) the main-chain oxygen atom of Ala107 and the nitrogen atom of the N-acetyl group of the reducing-end sugar residue in site C and (v) the Oδ1 atom of Asp101 and the O6 atom of the sugar residue in site B. These findings indicated that the replacement of Asn59 with Asp only minimally affects the affinity and the binding modes of the sugar substrates, even with the loss of two hydrogen bonds via water molecules (Fig. 3C). Instead, Asn59 is probably quite important for the catalytic activity. In the wild-type complex, Asn59 maintained the location of the side chain of the catalytic residue Asp52 in the well-ordered 'platform' hydrogen bonding network. The Asp59 mutant complex structure revealed the rearrangement of the platform hydrogen bonding network, with the concomitant loss of not only two water molecules but also eight hydrogen bonds (Fig. 3C), resulting in the slight movement of the Asp52 side chain (Fig. 3B). This could induce the improper structural orientation, and thus impair the catalysis.

DISCUSSION

Asp52 is one of the catalytic residues involved in the hydrolytic activity of the GlcNAc oligomer and bacterioglycan. It is considered to function by either stabilizing the oxocarbonium ion of the reaction intermediate or forming a covalent intermediate. Asn59 directly interacts with Asp52 in the well-ordered hydrogen bonding network on the 'platform' β-sheet, including Asp52 and Asn59 (Figs 2 and 3). However, there have been no structural or functional studies on the role of Asn59 in the hydrolytic activity. Here, we report the biochemical and crystallographic studies of the Asn59 mutant lysozymes. Unexpectedly, the introduction of only one methyl group

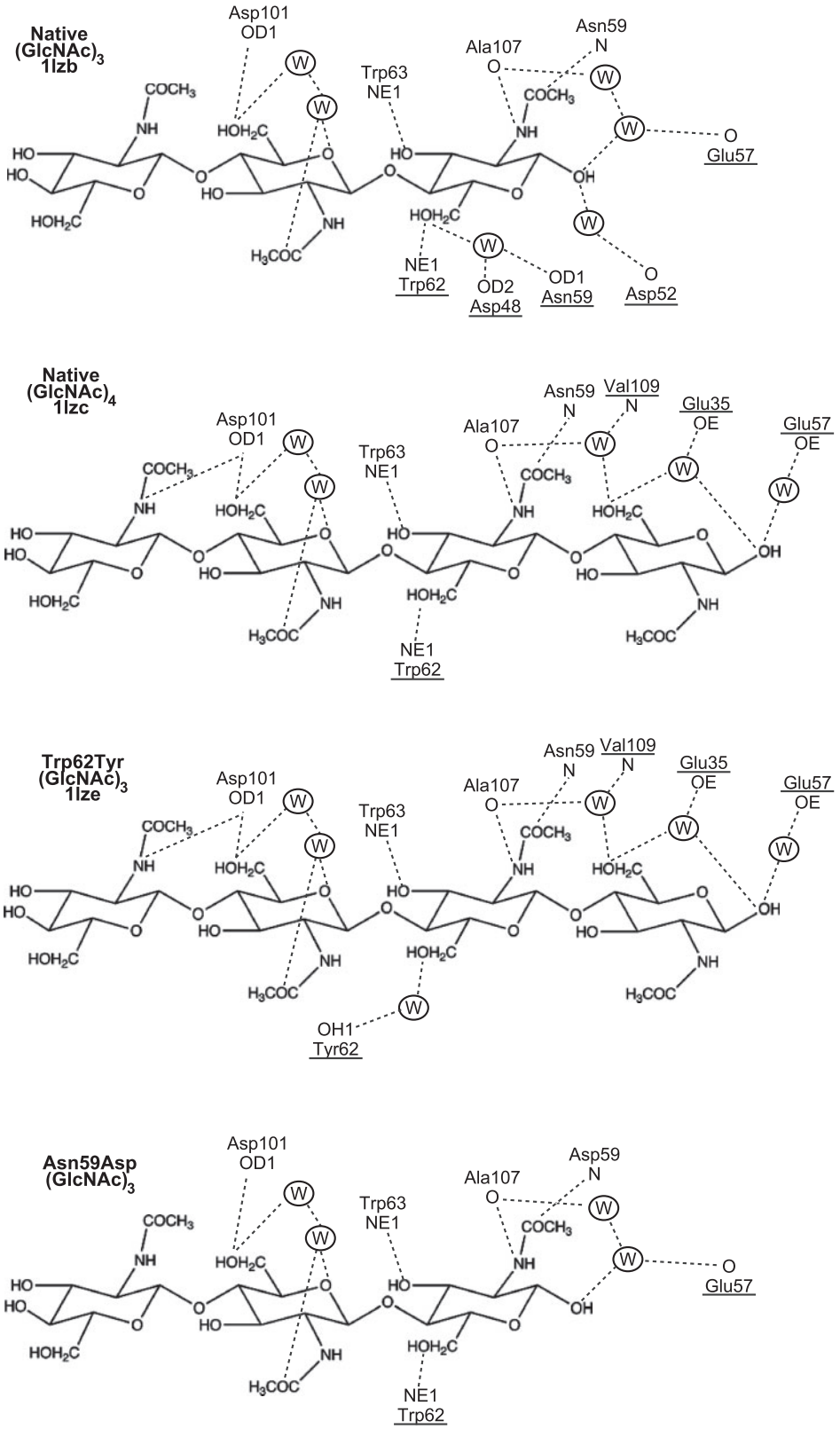

Fig. 4. **The interactions between the protein and the (GlcNAc)$_3$ or (GlcNAc)$_4$ molecule in the wild-type–(GlcNAc)$_3$, wild-type–(GlcNAc)$_4$, Trp62Tyr mutant–(GlcNAc)$_3$ and Asn59Asp mutant–(GlcNAc)$_3$ complex structures.** Amino acid residues with side chains participating in distinctive interactions in each structure are underlined.

to residue 59 (Asn59Gln mutation) significantly reduced the hydrolysis (<2% activity for the synthetic substrate PNP-$(GlcNAc)_5$ of the wild-type). Furthermore, the negative charge of Asp59 also exerted a detrimental effect on the hydrolytic activity for PNP-$(GlcNAc)_5$. The present crystal structure of Asn59Asp revealed that the orientations of the Asp52 and Asp59 side chains are changed significantly by the mutation, possibly because of the electrostatic differences in the residues, and thus Asp52 and Asp59 (~3.6Å) are too far apart to form a hydrogen bond (Fig. 3B). The significant change in the hydrogen bonding network system can also be evaluated by the fact that the Asp59 mutant–$(GlcNAc)_3$ complex structure loses two water molecules that exist in the wild-type enzyme–$(GlcNAc)_3$ complex structure (red spheres in Fig. 3C). These water molecules probably play significant roles in the stabilization of the hydrogen bonding network, by interacting with the side chains of Asp48, Asn46, Asp52 and Asn59 as well as the substrate sugar moieties (Figs 3C and 4). The water molecules may be eliminated by the flipping of the Asn46 side chain (Fig. 3C), caused by the mutation of the neighbouring Asn59. These results suggest that Asn59 contributes to the proper location of the side-chain of Asp52 for the enzymatic activity, by mediating the well-ordered hydrogen bonding network, including the water molecules.

On the other hand, the Asn59Gln mutation is also likely to induce remarkable changes of the hydrogen bonding network, but the addition of one methylene group by the Asn59Gln mutation presumably evokes distinct changes from those generated by the negative charge of the Asn59Asp mutation. Interestingly, we could not obtain the crystals of the Asn59Gln mutant, perhaps suggesting that the changes in the hydrogen bonding network induced by the Asn59Gln mutation may not be beneficial for the crystallization, in contrast to those generated by the Asn59Asp mutation.

We previously reported a series of biochemical, crystallographic and NMR studies of lysozymes in which the subsite B forming residues were mutated, *viz*., Trp62 and Asp101 (*14*, *20*, *21*), which are close to Asn59. The Trp62Tyr and Trp62Phe lysozyme mutants loosely bound the $(GlcNAc)_3$ molecule in both subsites A–B–C and B–C–D in the crystals, while the wild-type bound it in subsites A–B–C. Furthermore, the Trp62His/Gly and Asp101Gly mutant complexes revealed that the $(GlcNAc)_3$ molecule was hydrolyzsd via C–D–E or D–E–F. Its product, β-$(GlcNAc)_2$, was converted to α-$(GlcNAc)_2$ and accepted in an unproductive binding mode, L1–L2 (near site D), in the crystals. Therefore, the loss of the aromatic ring at position 62 disrupts both the stacking interactions and some hydrogen bonds with the substrate sugar, allowing the loose binding mode. In contrast, the present structural study of the Asn59Asp mutant complex showed that the Asn59 mutant, like the wild-type, exhibited the A–B–C binding mode for the $(GlcNAc)_3$ molecule. However, the mutants displayed minimal hydrolytic activity, clearly indicating that the Asn59 residue plays a pivotal role in the catalytic activity, rather than the substrate binding. As described above, the subtle conformational changes in both the side-chain and main-chain conformations of Asn59 caused the significant reduction in the hydrolytic activity. Previous mutagenesis studies of Asp52 demonstrated that the Asp52Glu and Asp52Ser mutations significantly reduced the hydrolytic activity, which also suggested that the precise location of Asp52 is necessary for efficient catalysis. Since this specific regulation of the hydrogen bonding network is important for the hydrolytic function, it would be interesting to assess the enzymatic activity of the Asn59Asp/Asp52Asn double mutant.

Taken together, Asn59 keeps the side chain of the catalytic residue Asp52 in the proper location, thus maintaining the extensive hydrogen bonding network on the 'platform'.

ACKNOWLEDGEMENTS

We thank Dr Kosuke Morikawa for his advice and encouragement, and Dr Shigeru Sugiyama, Dr Haiwei Song and Dr Daisuke Kohda for discussions.

FUNDING

Grant-in-aid for scientific research from the Ministry of Education, Culture, Sports, Science, and Technology of Japan (in part).

CONFLICT OF INTEREST

None declared.

REFERENCES

1. Wolfenden, R. (1969) Transition state analogues for enzyme catalysis. *Nature* **223**, 704–705
2. Jolles, P. and Jolles, J. (1984) What's new in lysozyme research? Always a model system, today as yesterday. *Mol. Cell Biochem* **63**, 165–189
3. Imoto, T., Johnson, L.N., North, A.C.T., Phillips, D.C., and Rupley, J.A. (1972) Vertebrate lysozyme in *The Enzyme* (Boyer, P.D., ed.) Vol. 7, 3rd edn, pp. 666–868, Academic Press, New York
4. Johnson, L.N., Cheetham, J., McLaughlin, P.J., Acharya, K.R., Barford, D., and Phillips, D.C. (1988) Protein-oligosaccharide interactions: lysozyme, phosphorylase, amylases. *Curr. Top. Microbiol. Immunol.* **139**, 81–134
5. Strynadka, N.C. and James, M.N. (1991) Lysozyme revisited: crystallographic evidence for distortion of an N-acetylmuramic acid residue bound in site D. *J. Mol. Biol* **220**, 401–424
6. Song, H., Inaka, K., Maenaka, K., and Matsushima, M. (1994) Structural changes of active site cleft and different saccharide binding modes in human lysozyme co-crystallized with hexa-N-acetyl-chitohexaose at pH 4.0. *J. Mol. Biol.* **244**, 522–540
7. Phillips, D.C. (1966) The three-dimensional structure of an enzyme molecule. *Sci. Am.* **215**, 78–90
8. Koshland, D.E. Jr. and Neet, K.E. (1968) The catalytic and regulatory properties of enzymes. *Annu. Rev. Biochem.* **37**, 359–410
9. Kuroki, R., Ito, Y., Kato, Y., and Imoto, T. (1997) A covalent enzyme-substrate adduct in a mutant hen egg white lysozyme (D52E). *J. Biol. Chem.* **272**, 19976–19981
10. Vocadlo, D.J., Davies, G.J., Laine, R., and Withers, S.G. (2001) Catalysis by hen egg-white lysozyme proceeds via a covalent intermediate. *Nature* **412**, 835–838

11. Inoue, M., Yamada, H., Yasukochi, T., Miki, T., Horiuchi, T., and Imoto, T. (1992) Left-sided substrate binding of lysozyme: evidence for the involvement of asparagine-46 in the initial binding of substrate to chicken lysozyme. *Biochemistry* **31**, 10322–10330
12. Kumagai, I., Maenaka, K., Sunada, F., Takeda, S., and Miura, K. (1993) Effects of subsite alterations on substrate-binding mode in the active site of hen egg-white lysozyme. *Eur. J. Biochem.* **212**, 151–156
13. Maenaka, K., Kawai, G., Watanabe, K., Sunada, F., and Kumagai, I. (1994) Functional and structural role of a tryptophan generally observed in protein-carbohydrate interaction. TRP-62 of hen egg white lysozyme. *J. Biol. Chem.* **269**, 7070–7075
14. Maenaka, K., Matsushima, M., Song, H., Sunada, F., Watanabe, K., and Kumagai, I. (1995) Dissection of protein-carbohydrate interactions in mutant hen egg-white lysozyme complexes and their hydrolytic activity. *J. Mol. Biol* **247**, 281–293
15. Tanaka, I., Yao, M., Suzuki, M., Hikichi, K., Matsumoto, T., Kozasa, M., and Katayama, C. (1990) An automatic diffraction data collection system with an imaging plate. *J. Appl. Crystallogr.* **23**, 334–339
16. Steigeman, W. (1974) Die Entwicklung und Anwendung von Rechenverfahren und Rechenprogrammen zur Strukturanalyse von Proteinen am Beispiel des Trypsin-Trypsininhibitor Komplexes, des freien Inhibitors und der L-asparaginase. *Thesis.* Technische Universitat, Munchen
17. Brünger, A.T., Adams, P.D., Clore, G.M., DeLano, W.L., Gros, P., Grosse-Kunstleve, R.W., Jiang, J.S., Kuszewski, J., Nilges, M., Pannu, N.S., Read, R.J., Rice, L.M., Simonson, T., and Warren, G.L. (1998) Crystallography & NMR system: a new software suite for macromolecular structure determination. *Acta Crystallogr. D* **54(Pt 5)**, 905–921
18. Murshudov, G.N., Vagin, A.A., and Dodson, E.J. (1997) Refinement of macromolecular structures by the maximum-likelihood method. *Acta Crystallogr. D* **53**, 240–255
19. Jones, T.A., Zou, J.Y., Cowan, S.W., and Kjeldgaard., (1991) Improved methods for building protein models in electron density maps and the location of errors in these models. *Acta Crystallogr. A* **47(Pt 2)**, 110–119
20. Maenaka, K., Matsushima, M., Kawai, G., Kidera, A., Watanabe, K., Kuroki, R., and Kumagai, I. (1998) Structural and functional effect of Trp-62 → Gly and Asp-101→Gly substitutions on substrate-binding modes of mutant hen egg-white lysozymes. *Biochem. J* **333(Pt 1)**, 71–76
21. Maenaka, K., Matsushima, M., Kawai, G., Watanabe, K., Kuroki, R., and Kumagai, I. (1998) Structural analysis of mutant hen egg-white lysozyme preferring a minor binding mode. *Biochim. Biophys. Acta* **1384**, 23–31